Analyst

TUTORIAL REVIEW

View Article Online
View Journal | View Issue

Cite this: *Analyst*, 2019, **144**, 2480

Fluorescent organic nanoparticles (FONs) as convenient probes for metal ion detection in aqueous medium

Mukhtiar Ahmed,[a] Muhammad Faisal,[a] Ayesha Ihsan[b] and Muhammad Moazzam Naseer*[a]

Recently, water contamination caused by metal ions has become one of the most serious problems as it has caused several deaths and socioeconomic problems around the world. Hence, the fast and accurate detection of metal ions in aqueous media has become the most important area of research; from time to time, new probes have been designed for this purpose. Among the previously reported sensors, probes based on fluorescent organic nanoparticles (FONs) have been gaining tremendous attention due to their ease of preparation/fabrication, synthetic diversity according to targeted metal ions, quick response, high selectivity toward different analytes at lower concentrations, tenable optical properties, and less toxicity. This review comprises two main sections, wherein we have tried to summarize the key progresses made in this field. The first section summarizes the literature dealing with FON-based chemosensors, which are used for the detection of transition metal ions of silver, copper, chromium, cadmium, mercury, iron, and zinc. The second section focuses on FON-based chemosensors that have been used for the detection of main group metal ions, namely, cesium, aluminum, strontium, lithium, and tin. Further, this review provides an adequate amount of information about the mechanism of metal ion sensing with FONs. It is expected that this review can provide sufficient information about this area of research and will be useful in fruitful progress in this field in the future.

Received 18th September 2018,
Accepted 21st February 2019

DOI: 10.1039/c8an01801d

rsc.li/analyst

1. Introduction

Metal ions play a very important role in life processes and they are used by all types of organisms to perform essential life functions.[1,2] It is estimated that in the human body, nearly 30% of enzymes use metal ions in some way.[3] In vital biological processes such as transmission of nerve impulses,[4] muscle contraction,[5,6] cell activity,[7] and other processes,[8,9] sodium, magnesium, potassium, and calcium play very important roles. In medicine, it is imperative to regulate the serum levels of lithium in patients under treatment for manic depression[10] and potassium in cases of high blood pressure.[11] The toxicity of aluminum has long been recognized and there is a controversy about its possible implication in Alzheimer's disease.[12,13] In chemical oceanography, it has been verified that certain nutrients are absolutely necessary for the survival of microorganisms in seawater, such as zinc, iron, and manganese.[14,15] In spite of the fact that metal ions are very essential for sustaining life, their extensive use can cause serious health and environmental issues. For example, certain heavy metal ions such as Fe^{3+}, Zn^{2+}, Cu^{2+}, Co^{2+}, Mn^{2+}, and Mo^{6+} and their higher concentrations can mainly cause several serious health problems.[16,17] Further, there are certain other heavy metal ions, namely, Hg^{2+}, Cd^{2+}, Pb^{2+}, and As^{3+}, which are investigated as highly toxic ions and are responsible for numerous health issues.[18] Accordingly, the determination of trace amounts of metal ions is of increasing interest in several fields such as environmental analysis, process control, biology, medicine, *etc.*

So far, several methods such as atomic absorption/emission spectroscopy,[19–21] inductively coupled plasma mass spectroscopy,[22,23] inductively coupled plasma atomic emission spectroscopy,[24] electrochemical assays,[25] Auger electron spectroscopy,[26] polarography,[27] and recently formulated colorimetric methods[28,29] have been developed for the detection of metal ions. Their practical applications are inadequate because these techniques need sophisticated instrumentation; however, in the last two decades, fluorescent-mediated probes to detect metal ions have gained tremendous attention owing to their promising photophysical properties. For instance, their fluorophores can be altered by several ways: charge trans-

[a]*Department of Chemistry, Quaid-i-Azam University, Islamabad 45320, Pakistan. E-mail: moazzam@qau.edu.pk*
[b]*Nanobiotechnology group, National Institute for Biotechnology and Genetic Engineering (NIBGE), P.O. Box 577, Jhang Road, Faisalabad, Pakistan*

fer, electron transfer, energy transfer, influence of metal ions, and destabilization of nonemissive n–π* excited states.[30,31]

Subsequently, many fluorophores have been used for sensor improvement in the past, but problems like narrow excitation spectra and broad emission spectra are associated with such fluorophores;[32] further, these probes work exceptionally well in organic solvents, but have limited applications in aqueous media.[33] Sensor activities in nonaqueous media sometimes restrict their use in real-life applications, for example, in environmental and biological samples. However, in recent times, fluorescent organic nanoparticles (FONs) have been progressively used to overcome the shortcomings of traditional fluorogenic sensors for cations. FON-based probes are more beneficial as compared to traditional fluorophores due to their tenable photoluminescence, promising assortment of flexibility in material synthesis, good water solubility, availability of organic molecules, superiority of biodegradation, biocompatibility, photostability, and optical properties depending upon the size of the nanoparticles.[34,35] Further, most of the fluorescent chemosensors are used in solution because of which they suffer from problems such as blinking, photobleaching, and intractable self-quenching. By comparison, FONs are a new class of chemosensors that provide additional results as compared to molecule-based probes. Some FONs show the aggregation-induced emission enhancement (AIEE) effect. The active AIEE molecules have a generic feature in which they exhibit low or no fluorescence when freely dissolved in a solvent. However, upon the addition of a solvent (which reduces their solubility), the fluorescence intensity drastically increases as a result of aggregate formation.[36] These nanosensors are easy to fabricate and require less synthesis labor as compared to traditional water-soluble sensors. Normally, these nanosensors are fabricated by employing a single-step re-precipitation technique, but other important approaches such as emulsion polymerization, sol–gel phase transition, laser ablation, stratification deposition, and solvent evaporation have also been employed.[37–41] By realizing the importance of FONs as sensors for metal ions in aqueous media, we aim to provide a brief understanding of this field. We have tried to cover the major reports of these types of sensing platforms and hope that this will facilitate the progress in this field.

2. Mechanism of sensing metal ions using FONs

Metal ions when detected by FONs *via* the technique of fluorescence necessitate certain obvious changes in the fluorescence emission by the fluorophore. In order to achieve this, there are three important ways: (i) fluorescence enhancement, (ii) fluorescence quenching, and (iii) shift in emissions. Fluorescence enhancement involves the employment of a fluorophore that enhances its fluorescence or becomes fluorescent in the presence of metal ions and has little or no fluorescence in the absence of metal ions. The increase in the fluorescence of such a receptor fluorophore is mainly due to the induced conformational restriction that results from the binding of metal ions. Fluorescence quenching involves the selection of molecules that exhibit high fluorescence in the absence of metal ions but their fluorescence suddenly vanishes or considerably reduces in the presence of the target metal ions. Finally, emission changes mainly depend upon the shift in the emission band of the fluorophore upon interaction with specific metal ions; the resultant shift in the band may be at a higher or lower wavelength. In this case, the change in the emission maximum is mainly due the reaction of the metal ions with the fluorophore and results in new molecules with new emission maxima.[1,9] These changes may be attributed to photoinduced electron transfer (PET), intramolecular charge transfer (ICT), and photoinduced charge transfer (PCT). The enhancement in fluorescence is termed as chelation-enhanced fluorescence (CHEF); contrarily, the decrease in fluorescence is termed as chelation-enhanced fluorescence quenching (CHEQ). As the metal ions from the main groups possess high charge density and high electropositivity, when these ions are complexed with the receptor, it causes an enhancement in the fluorescence of the receptor[42] *via* the inhibition of PET; however, most of the transition metals are known to be fluorescence quenchers because they have the ability to quench fluorescence by the energy transfer mechanism. There are other more frequent mechanisms observed in metal detection *via* fluorescence changes. The other common mechanisms observed during sensing metal ions are Förster resonance energy transfer (FRET), fluorescence resonance energy transfer (FRET), resonance energy transfer (RET), and electronic energy transfer (EET). He *et al.* described additional details about the mechanisms involved in sensing metal ions.[43] Such mechanisms for sensing depend upon the interaction of metal ions with the binding sites of sensors; therefore, the mechanism of sensing metal ions with FONs is the same as that when using traditional sensors; however, in some cases, metal ions adsorb on the surface of the nanoparticles, which results in the alteration of the photophysical properties of the molecule and a change in the fluorescence signatures is observed. Further, the self-assembly of these nanoaggregates allows the formation of binding sites for metals on the surface of the nanoparticles, which facilitates the increased efficiency and sensitivity of these nanosensors towards metal ions as compared to those of traditional water-soluble sensors.

3. FON-based chemosensors for transition metal ions

3.1 FON-based chemosensors for silver ions

Silver is considered to be a silent ion that does not have any spectroscopic signals due to which it is difficult to discriminate it from other correlated metal ions.[44] Recently, only fluorescence detection techniques have been preferred for the detection of such silent hazardous metal ions.[45] Yan *et al.* synthesized molecular probe **1** based on triazolo-thiadiazole; the

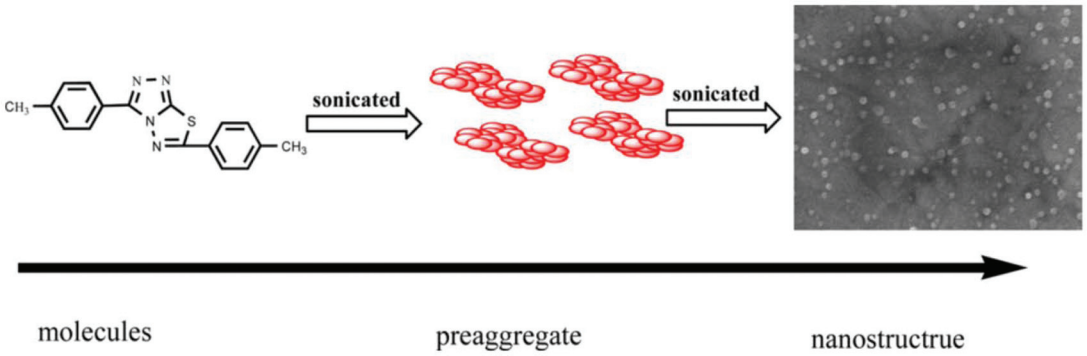

Fig. 1 Schematic representation of the formation process of nanoscale materials of **1**. Adapted with permission from ref. 46. Copyright 2011 Elsevier Ltd.

synthesized probe was fabricated into nanoparticles to maximize its use in aqueous environments (Fig. 1).[46] After the addition of excess Ag^+ (6.7 equiv.) in the aqueous solution of **1**, a 1.95-fold emission enhancement was observed, whereas no fluorescence increase was observed for other interfering metal ions (Fig. 2). The obvious change in the fluorescence of **1** upon interaction with silver ions was due to the formation of a complex between the silver ions and **1**, which resulted in the inhibition of the PET phenomenon. The proposed nanoreceptor showed high sensitivity toward silver ions with the limit of detection (LOD) of 2.58×10^{-7} M. Similarly, for the detection of silver ions in aqueous media, a ratiometric dipodal nanosensor based on imine-linked 1,8-naphthalimide **2** was fabricated by Sharma *et al.*[47] The addition of Ag ions caused selective ratiometric changes (quenching at 522 nm and enhancement at 627 nm) in the emission profile of nanoreceptor **2** in the presence of other interfering metal ions (Fig. 4). The ratiometric changes in this nanoreceptor were caused by the interaction of Ag ions with the naphthalimide rings of the nanoreceptor, which causes π–π stacking and results in the formation of "excimers." Furthermore, the receptor displayed a linear response toward silver ions over a large range of pH (2.3–12.3), with a lower LOD value (15.5 nm) and shorter response time (84 s).

According to the hard and soft acids and bases (HSAB) principle, Ag ions prefer to bind with soft nucleophiles;[48,49] based on this strategy, several fluorescent probes have been designed for the detection of Ag ions, most of which are based on thiourea derivatives.[28] This is because thiocarbonyl present in the thiourea moiety acts as a soft site for the binding of Ag ions. Most of the times, Hg^{2+} —a soft electrophile— causes interference in the determination of Ag^+. For example, thiourea containing naphthalene–thiadiazole **3**-based FONs displayed selective fluorescence quenching upon interaction with silver ions with marginal interference from Hg^{2+} (Fig. 4). Quenching in the fluorescence of the nanoreceptor can be attributed to the formation of small Ag nanoparticles on the surface of the nanoreceptor. The proposed nanosensor exhibited a linear response over a wide concentration range of silver ions with LOD of 4.7×10^{-8} M (5 ppb) (Fig. 3).[50]

Recently, Navneet Kaur and co-workers fabricated a highly efficient, noninvasive, and economical fluorescent chemosensor mediated on organic nanoparticles (ONPs) of Biginelli compound **4** for the selective detection of Ag^+ spermidine

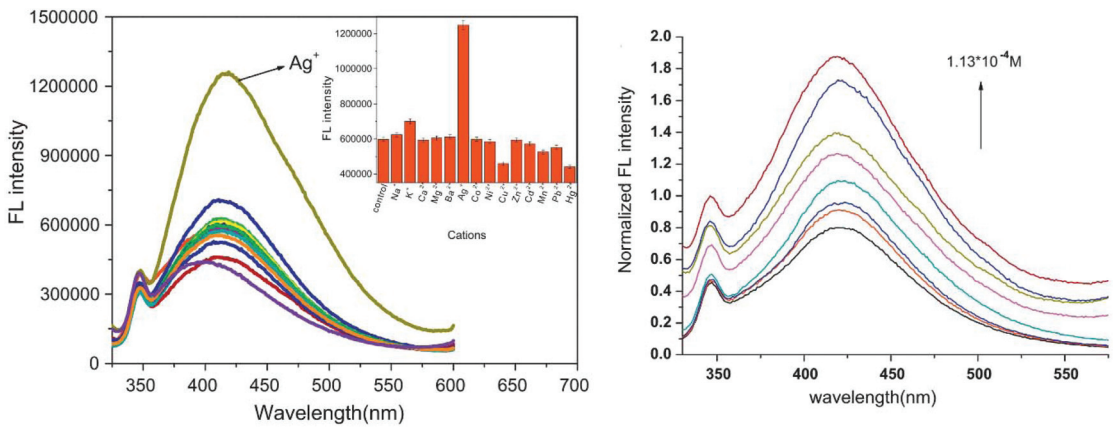

Fig. 2 Fluorescence emission spectra of FONs (7.5×10^{-6} M) with or without various cations and plot of the fluorescent intensity as a function of Ag^+ concentration. Adapted with permission from ref. 46. Copyright 2011 Elsevier Ltd.

Fig. 3 Photographs of FON solutions after adding 5×10^{-4} M of the indicated metal ions after 24 h and the schematic illustration of the possible structure of Ag-nanoparticle-coated **3** aggregates. Adapted with permission from ref. 50. Copyright 2008 Elsevier Ltd.

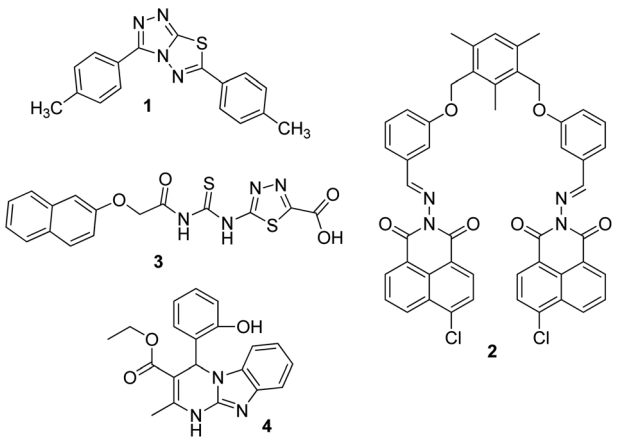

Fig. 4 Structures of FONs for the detection of silver ions.

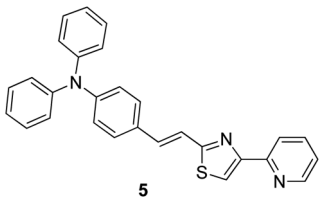

Fig. 5 Structure of nanoreceptor (*E*)-*N*,*N*-diphenyl-4-(2-(4-(pyridin-2-yl)thiazol-2-yl)vinyl)aniline **5**.

cations in biological samples (urine) and in environmental samples (river water) by quenching of fluorescence emissions (Fig. 4).[51] The LOD was observed to be 7.9 nM for Ag^+. The nanosensor involving Biginelli compound **4** could be applied in a broad spectrum of pH (3–12); hence, it was suitable for ion investigations in physiological and environmental conditions.

3.2 FON-based chemosensors for copper ions

Copper is an important micronutrient that is imbibed by the human body along with food and water: a daily intake of 2 mg of copper has been recommended by the U.S. Food and Drug Administration (FDA). Besides the advantages of copper, its extensive use can result in gastrointestinal problems and kidney failure.[52] Because of the paramagnetic nature of Cu^{2+}, most of the times, it causes quenching of fluorescence emission of chemosensors and leads to a turn-off signal.[53]

Compound **5** based on rigid conjugated pyridinylthiazole derivatives was synthesized and fabricated into nanoparticles for the selective detection of Cu^{2+} ions in aqueous media by Hou *et al.*[54] The fluorescent intensity of the nanoreceptor showed an inverse relationship with the addition of Cu^{2+} ions; however, it remained unchanged with other competing metal ions (Fig. 5). Compound **5** nanoparticles, as compared to their monomers, displayed additional fluorescence sensitivity toward Cu^{2+} ions. The dynamic working of Cu^{2+} ions is exhibited by the proposed nanosensor ranges from 0.02 to 0.50 μM having LOD of 10 nM; however, the direct measurement of Cu^{2+} ions in the sample of drinking water has been expressed by planned chemosensors with satisfactory results.

Recently, certain polymer-based fluorescent nanoprobes have been gaining considerable attention because of their possible use as detectors for metal ions.[55] Based on this, Chen *et al.*[56] proposed a multifunctional fluorescent nanosensor based on FRET. Fluorescent polymer nanoparticles were synthesized *via* the copolymerization of estrone, vinylbenzyl chloride, and fluorescent vinylic cross-linking monomer (fluorescein-*o*,*o*-bis-propene (FBP)) in oil-in-water mini-emulsion, stabilized with cationic surfactant (dodecyltrimethylammonium bromide (DTAB)). Finally, 1,4,7,10-tetraazacyclododecane (cyclen) was grafted onto the surface of the nano-

particles, which acts as a ligand for potential binding with metal ions. The fabricated polymeric nanoparticles exhibited very selective "on–off" response toward Cu^{2+} among 11 other common interfering metal ions in a pure aqueous medium. The selectivity of the proposed polymeric nanoreceptor toward Cu^{2+} was due to FRET between the FBP and Cu^{2+}-cyclen complex. The polymeric nanosensor exhibited a very sensitive response toward Cu^{2+} ions and responded to very low concentrations up to 340 nM. A similar approach was reported by Su *et al.* who investigated a "turn-off" nanoprobe based on polydihydroxyphenylalanine nanoparticles (PDNPs) for the fluorescent detection of Cu^{2+} in aqueous media. Under optimized conditions, the nanoprobe showed a selective response toward Cu^{2+} *via* a decrease in the fluorescence intensity at 520 nm; no other common interfering cations caused any changes in the emission profile of the nanoreceptor. The nanoreceptor exhibited high sensitivity toward Cu^{2+}, with LOD of 0.10 μM, which is well below the safety limit of Cu^{2+} in drinking water permitted by the U.S. Environmental Protection Agency (EPA). Furthermore, the scope of detection of the nanosensor toward Cu^{2+} in river water samples was extended with satisfactory results.[57]

3.3 FON-based chemosensors for chromium ions

Usually, chromium exists in the form of two oxidation states, *i.e.*, trivalent and hexavalent states. Here, Cr^{3+} is a vital trace element, and it plays an important role in the action of insulin and glucose, protein, and lipid metabolism. However, Cr^{6+} is dangerous to health and can cause damage to the human gastrointestinal, hematological, respiratory, immunological, developmental, and reproductive systems.[58] Recently, the detection of this hazardous metal ion *via* fluorescence changes has become pivotal because this ion may induce changes in the photophysical properties of the receptors when they are complexed with it. These two suspected ions can be selectively detected in the presence of each other. A fluorescent sensor based on 3-aminopropylmethyl (tetra phenyl) silole **6** nanoparticles was synthesized by Trogler and co-workers (Fig. 7)[59] for the selective detection of Cr^{6+} in aqueous media. When excited at 360 nm, the nanosensor exhibited an emission at 485 nm. The fluorescence of the sensor selectively declines with Cr^{6+} with a marginal effect of As^{5+}. The mechanism of quenching was supposed to be a result of electron transfer from the excited state of the silole to the analyte. Not surprisingly, since AsO_4^{3-} is a weaker oxidant than CrO_4^{2-}, it is a weaker quencher, too (standard reduction potentials *vs.* NHE are −0.68 and −0.13 V, respectively; at pH 7, they are +0.15 and +0.56 V, respectively).

Dalavi *et al.*[60] fabricated a very efficient fluorescent nanosensor based on cetyltrimethylammonium bromide (CTAB)-stabilized perylene nanoparticles (PNPs) for the selective detection of Cr^{6+}. Under the most opportune conditions, the fluorescence intensity of PNPs examined at an excitation wavelength of λ_{max} = 382 nm was quenched by the consecutive addition of growing concentrations of dichromate ions (Fig. 6). Fluorescence quenching was a result of the alteration of the surface of monodisperse nanoparticles that was restricted with dichromate ions by electrostatic interactions to form stable nonfluorescent micelle complexes in the ground state. The sensor could detect target cations with concentrations as high as 0.008 mg mL^{-1}. Furthermore, this method of sensing was highly appreciable with promising results for the detection of contents of Cr^{6+} in synthetic and environmental samples.

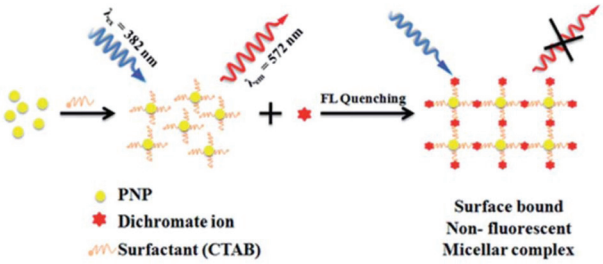

Fig. 6 Proposed mechanism for the formation of CTAB PNPs and surface-bound stable nonfluorescent micellar complexes with dichromate ions. Adapted with permission from ref. 60. Copyright 2014 the Royal Society of Chemistry.

Similarly, Wang *et al.* carried out the fabrication of ONPs based on anthracene/polyacrylamide (AN/PAM) for the selective determination of Cr^{6+} in aqueous media. Under optimum conditions, the excitation spectra of AN/PAM nanoparticles have their maximal peak at 345 nm, which shifts to 405 nm with a concomitant increase in intensity after the addition of Cr^{6+} and linearly reduces with the addition of higher concentrations of Cr^{6+}. Under optimum conditions, numerous common cations such as Na^+, K^+, Mg^{2+}, Al^{3+}, Fe^{3+}, Ca^{2+}, Zn^{2+}, Cr^{3+}, Hg^{2+}, Cu^{2+}, Co^{2+}, Ni^{2+}, Ag^+, Mn^{2+}, and Sn^{2+} were tested for their possible interference, but none of the metal ions posed any interference in the determination of Cr^{6+}. In addition, from these fluorescence studies, it was evident that the planned nanoprobe could detect Cr^{6+} with LOD as low as 0.02 μg ml^{-1}. The subsequent addition of Cr^{6+} causes the gradual oxidation of PAM and reduction of Cr^{6+} into $Cr(OH)_3$. The oxidative product of PAM reduces the fluorescence intensity; further, $Cr(OH)_3$, which enveloped the nanoparticles, also decreased a portion of the fluorescence, which eventually resulted in the reduction in fluorescence with an increase in Cr^{6+} concentration.[61] A nanoprobe based on 1,8-naphthalic anhydride and triethylenetetramine ligand **7** was synthesized and fabricated into its nanoparticles by Saini and co-workers for the selective detection of Cr^{3+} in aqueous media (Fig. 7). The proposed nanosensor exhibited selective enhancement in the emission intensity in the presence of targeted metal ions. The enhancement in the emission was due to the complexation of Cr^{3+} with the nitrogen part of triethylenetetramine, which resulted in the inhibition of PET. Furthermore, the nanoprobe showed high selectivity toward Cr^{3+} with LOD of 64 nM.[62]

Pyrene and its derivatives are well known for their brilliant optical properties,[63] and they have been used in several sensing platforms as a fluorophore core.[42,64] On the basis of

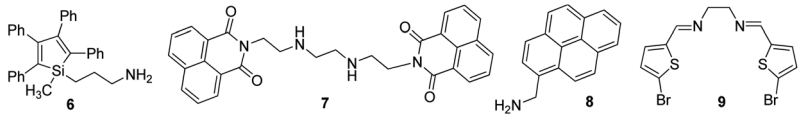

Fig. 7 Structure of chemosensor for the fluorescent detection of chromium ions.

the importance of pyrene as a fluorophore, Wang *et al.*[65] converted 1-pyrenemethylamine **8** into its nanoparticles for the selective detection of Cr^{6+} in water. The sensor displayed the maximum excitation and emission at 238, 283, 351, 383, and 400 nm, but only λ_{ex} = 238 and λ_{em} = 400 nm were selected for the recognition studies (Fig. 7). The fluorescence of the nanosensor was quenched with the successive addition of Cr^{6+}, but remained unchanged with other common interfering metal ions. From these fluorescence studies, it was evident that the sensor could detect Cr^{6+} ions up to concentrations of 2.8×10^{-6} mol L^{-1}. In 2018, Viviana *et al.* developed an efficient technique for the recognition of Cr^{3+} in water and multivitamin formulations by employing fluorescent nanosensors mediated on *N*,*N*′-bis(5-bromo-2-thiophenylmethyl)ethylenediimine (BTED **9**).[66] BTED-based nanosensors selectively and sensitively identify Cr^{3+} cations without detecting other coexisting metal cations in a H_2O bath and aqueous vitamin tablets. The LOD was observed to be 7.3 μM.

Recently, imine-linked fluorophores have gained considerable attention for metal ion recognition due to the ease of operation afforded by excited state intramolecular proton transfer (ESIPT), high fluorescence yield, and dual channel emission with keto–enol tautomerism (Fig. 8).[67,68] Based on this strategy, Kaur *et al.*[32] designed the synthesis of glutathione-based tripeptide and imine-linked fluorescent sensor **10** *via* the condensation reaction between salicylaldehyde and tripeptide glutathione (GSH). The synthesized fluorescent sensor was fabricated into nanoparticles for the selective detection of Cr^{3+} in an aqueous bath. When excited at 324 nm, because of keto–enol tautomerism, the sensors exhibited two emission peaks at 369 and 400 nm (Fig. 9). The emission peak at 369 nm revealed enhancement in the fluorescence intensity upon the addition of Cr^{3+}; however, the emission peak at 490 nm gets quenched. Other metal ions have a negligible influence on the sensing system under the same conditions. The fluorescence enhancement at one wavelength (369 nm) and quenching at the other (400 nm) can be explained on the basis of local field enhancement and radiationless energy transfer process between the metal and the host. When the metal is attached to the host, the local field causes the stimulation of molecules, which consequently leads to enhancement in fluorescence intensity. Further, when the energy loss occurs toward the metal, fluorescence quenching takes place. The nanosensor displayed a linear response for Cr^{3+} over a wide concentration range (0.55–50 μM) with LOD of 0.25 μM.

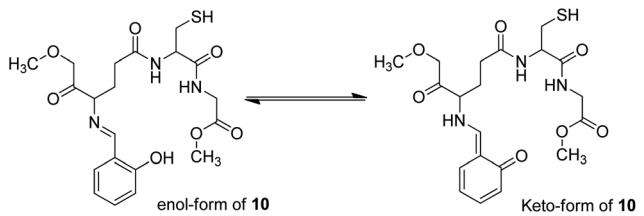

Fig. 8 Keto–enol tautomers of probe **10**.

3.4 FON-based chemosensors for cadmium ions

Cadmium concentration in drinking water is 0.005 mg L^{-1} or 4.4×10^{-8} M, which is declared by the EPA. Malfunctions may be caused by the long-term exposure to cadmium for the abovementioned levels. Mahajan *et al.*[69] demonstrated that *N*-methyl isatin nanoparticle (*N*-MINPs) **11** was used as selective fluorescent sensors for Cd^{2+} ions in aqueous media (Fig. 10). Under optimized conditions, the emission of the nanosensor increased with the addition of Cd^{+} ions; however, a contradictory response was observed for other metal ions,

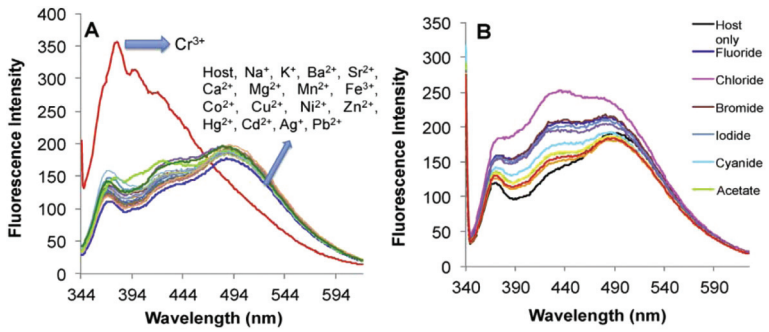

Fig. 9 Changes in the fluorescence spectrum of **10** (FONs) (20 M) in aqueous medium upon the (A) addition of 50 M of a particular metal nitrate salt in an aqueous medium and (B) addition of 50 M of a particular anion as tetrabutylammonium salt in an aqueous medium. Adapted with permission from ref. 32. Copyright 2015 Elsevier Ltd.

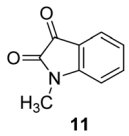

11

Fig. 10 Structure of fluorescent chemosensor 1-methylindoline-2,3-dione **11**.

namely, Ni^{2+}, Cu^{2+}, Hg^{2+}, Sn^{2+}, Pb^{2+}, Ca^{2+}, Zn^{2+}, Na^{+}, K^{+}, Co^{2+}, and Mg^{2+}. Cadmium is a soft metal and forms a complex with *N*-MINP ligands by electrostatic forces originating from oxygen that functions as the donor group of carbonyl functionality (Fig. 11). The formation of a rigid complex leads toward the restriction in free rotation of the carbon in the carbonyl group with respect to the indole ring, ultimately causing an increase in the fluorescence intensity of the receptor. The fabricated nanosensor was found to be very sensitive toward Cd^{2+} as it could detect ion concentrations as high as 1.33 μg mL^{-1} (Fig. 12).

3.5 FON-based chemosensors for mercury ions

Bhardwaj *et al.* proposed the synthesis and fabrication of dipodal-rhodamine-based fluorescent nanoprobe **12** for the selective detection of Hg^{2+} ions in aqueous media (Fig. 6). When excited at 530 nm, the nanoprobe did not exhibit any fluorescence with most metal ions; however, a new band at 547 nm appeared when Hg^{2+} (10 μM) was added, with almost 100 times increase in the fluorescence intensity (Fig. 13).[70] The sensor displayed a linear response toward Hg^{2+} over a wide concentration range (0 μM to 730 μM) with LOD of 0.1 nm. The enhancement in the fluorescence of the receptor can be attributed to the spirolactam ring opening assisted by the coordination of Hg^{2+} (Fig. 14).

Thiourea-based tripodal nanoreceptor **13** was fabricated by Singh and co-workers for the detection of Hg^{2+} in aqueous media (Fig. 16).[71] The addition of Hg^{2+} ions cause selective enhancement in the fluorescence of nanoreceptors in the presence of other common interfering metal ions. This can be attributed to the binding ability of Hg^{2+} with a nanoreceptor that rearranges the framework into static conformation

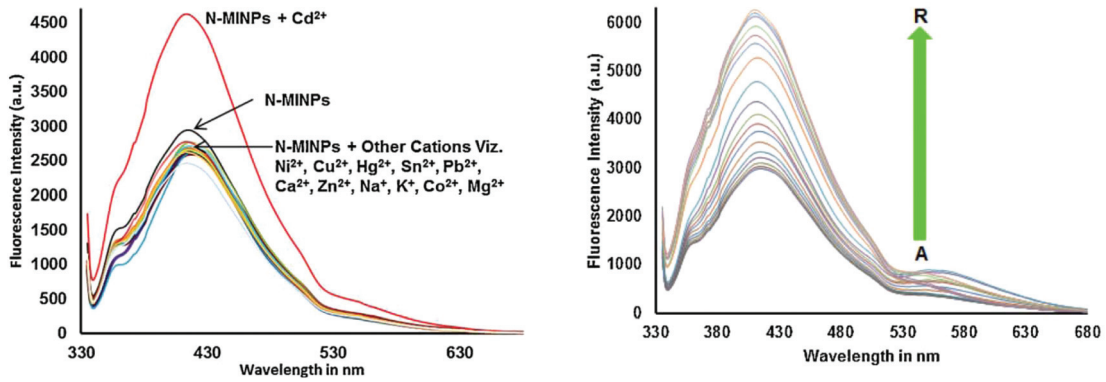

Fig. 11 Selectivity of **11** toward Cd^{2+} shows fluorescence enhancement as compared to other cations, and the fluorescence spectra of *N*-MINP suspension (1×10^{-5} M) in the presence of different concentrations of Cd^{2+} ions. Adapted with permission from ref. 69. Copyright 2015 Elsevier Ltd.

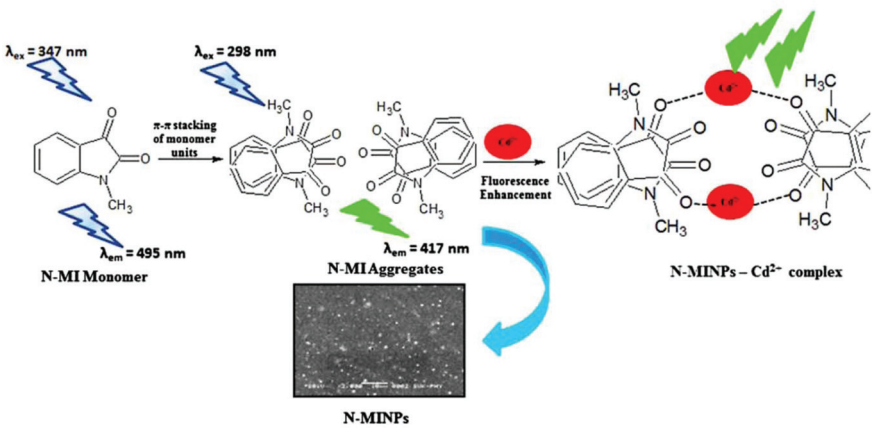

Fig. 12 Proposed graphic for the formation of **11** and its complexation with Cd^{2+} ions. Adapted with permission from ref. 67. Copyright 2015 Elsevier Ltd.

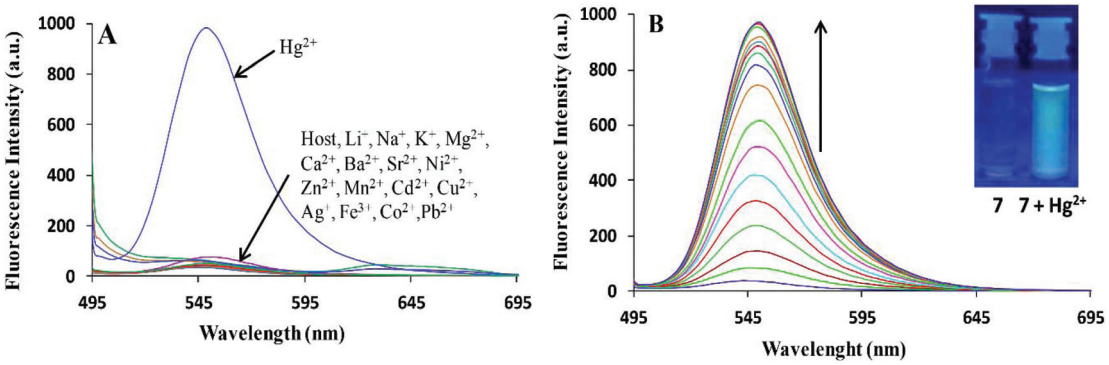

Fig. 13 (A) Changes in the fluorescence emission spectra of 195 nM solution of **12** (FON) upon the addition of 10 μM of different metal ion salts in 15 aqueous media; (B) changes in the fluorescence emission spectra of 195 nM solution of **12** (FON) upon the successive addition of 0 to 10 μM of Hg^{2+} in an aqueous medium. Adapted with permission from ref. 70. Copyright 2013 the Centre National de la Recherche Scientifique (CNRS) and the Royal Society of Chemistry.

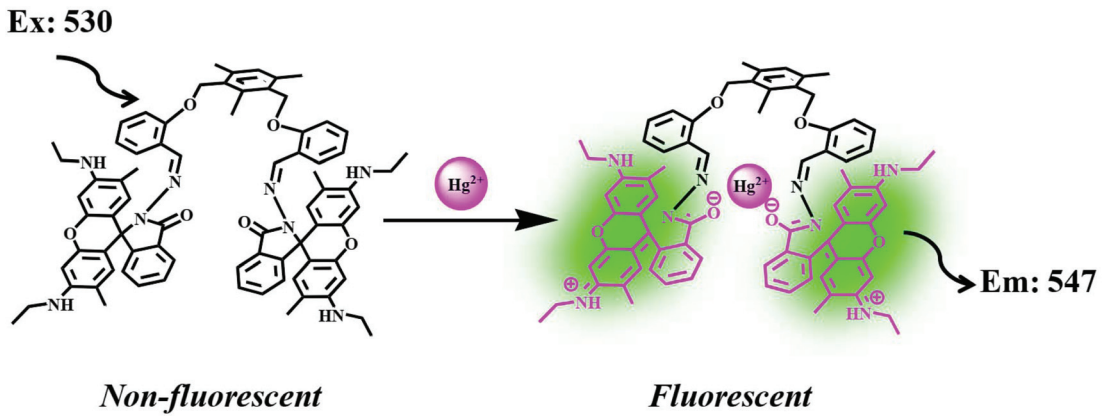

Fig. 14 Process of sensing through the coordination of Hg^{2+}. Adapted with permission from ref. 70. Copyright 2013 CNRS and the Royal Society of Chemistry.

through multivalent interactions, ultimately yielding PET. The nanoreceptor exhibited a linear response toward Hg^{2+} over a wide concentration range of 0–10 μM with LOD of 2.4 nM (Fig. 15). Similarly, Li and Yan[72] proposed a ratiometric fluorescent probe based on thiourea–thiadiazole–pyridine-linked **14** FONs for the selective recognition of Hg^{2+} ions (Fig. 16). Upon binding with Hg^{2+}, the nanoreceptor exhibited a 46-fold increase in the fluorescence quantum yield along with a 98 nm red-shift in the fluorescence emission. The observed variation in fluorescence can be attributed to the potential of Hg^{2+} to convert theorem into urea.[73] Under optimum conditions, the sensor showed LOD of 1.13×10^{-7} M (22.6 ppb); however, other metal ions, namely, Ni^{2+}, Cd^{2+}, Ca^{2+}, Na^{+}, Cu^{2+}, Ag^{+}, Pb^{2+}, Mg^{2+}, and Mn^{2+}, did not induce any significant variation in the emission profile of the sensor.

Biginelli-based compounds **15**, **16**, and **17** were synthesized by Singh *et al.*[74] and fabricated into nanoparticles to test as a selective sensor for metal ions in aqueous media (Fig. 16). Upon the addition of suspected cation solution (100 μM) to the aqueous solution of nanoreceptors (20 μM), only nanosensor **16** exhibited a selective response to Hg^{2+} ions. The addition of Hg^{2+} resulted in the quenching of the emission band at λ_{max} = 456 nm and an enhancement in λ_{max} to 440 nm. The binding of Hg^{2+} with the nanoreceptor caused a disturbance in the electron cloud of the fluorophore, thereby resulting in PET; this ultimately resulted in a decrease in the emission with a blue-shift. The nanosensor displayed a very sensitive response toward Hg^{2+} ions over a wide concentration range (0–100 μM) with LOD of 1 nM.

The nanoparticles of a fluorescent polymer based on 2-vinylnaphthalene and acrylic acid were fabricated by Wang *et al.*[75] *via* ultrasonic radiation. These polymer-based nanoparticles were used for the detection of Hg^{2+} in aqueous media. The nanoprobes presented excellent sensing potential toward Hg^{2+} ions, since the probes could detect suspected ions as high as 0.01 μg ml^{-1}. The utility of the nanosensor was also evaluated with artificial samples, and the sensor yielded satisfactory results. Similarly, Wang *et al.* developed polymer-mediated fluorescent ratiometric nanoprobe NP3 for the selective detection of Hg^{2+} ions in water. The NP3 nanoprobe contains a reference fluorescent dye (EANI *viz.* 4-ethoxy-9-allyl-1,8-naphthalimide **18**) that resides in the nucleus of the nano-

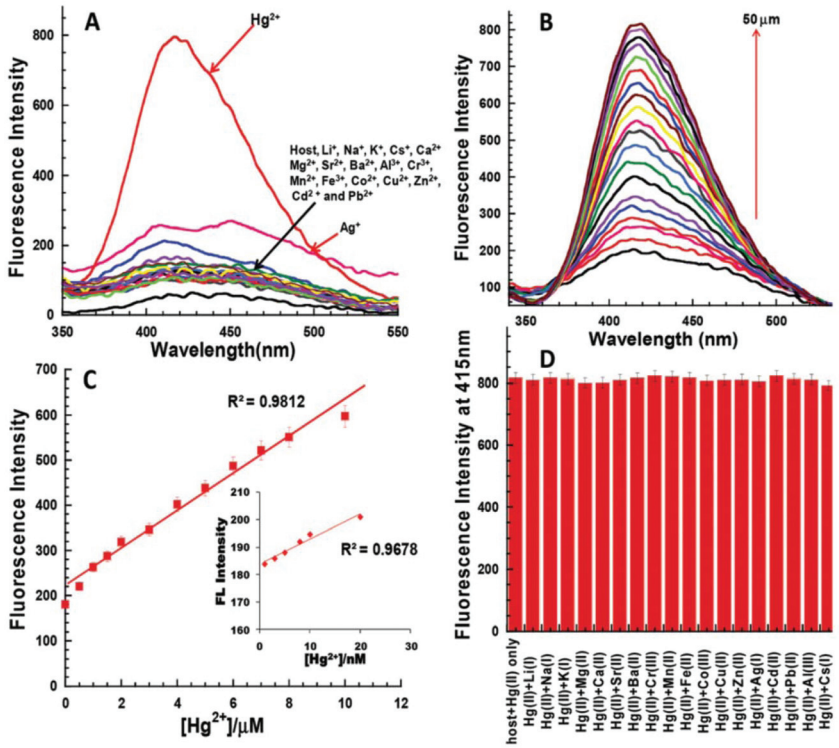

Fig. 15 (A) Changes in the emission profile of nanoaggregates **13** (10 μM) in water upon the addition of 50 μM of a particular metal nitrate salt; (B) changes in the emission profile of nanoaggregates **13** (10 μM) upon the successive addition of Hg^{2+} (0–50 μM); (C) linear regression graph between the concentration of added mercury ions (0–10 μM) and increase in the fluorescence intensity of nanoaggregates **13** (25 μM). Inset: Linear regression plot of nanoaggregates **13** (10 μM) and addition of Hg^{2+} in the range of 0–20 nM; (D) influence of other metal ions on Hg^{2+}-based changes in the emission profile of nanoaggregates **13**. Adapted with permission from ref. 71. Copyright 2014 the Royal Society of Chemistry.

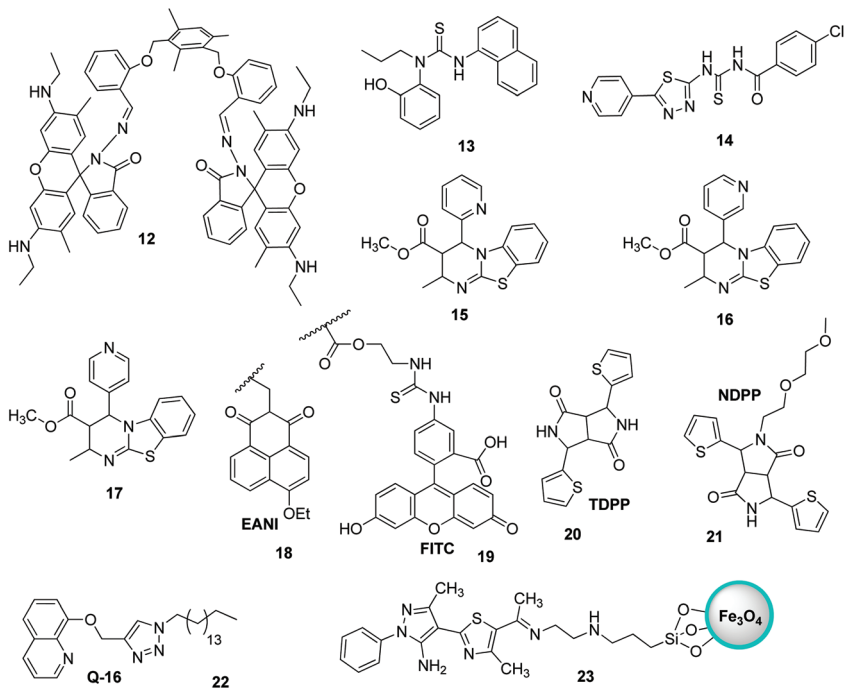

Fig. 16 Structures of FON-based chemosensors for the detection of mercury ions.

sensor, and the Hg^{2+} identification system (FITC, *i.e.*, fluorescein derivative **19**) is present on the exterior of the nanosensor (Fig. 16).[76] The nanoprobe exhibits excellent long-term photostability, promising H_2O dispersibility, and highly sensitive and selective ratiometric recognition of Hg^{2+} ions in H_2O relative to other interfering cations, namely, Fe^{2+}, Ag^{+}, Cd^{2+}, Fe^{3+}, Ca^{2+}, K^{+}, Mn^{2+}, Co^{2+}, Zn^{2+}, Mg^{2+}, Na^{+}, and Cu^{2+}, as well as reasonably low LOD (~75 nM). In 2017, Nie *et al.* investigated the fluorescent recognition of Hg^{2+} ions in water by using two organic DPP-mediated sensors, namely, TDPP- and NDPP-mediated loose micelle-type nanosensors.[77] Commercially available TDPP **20** having NH entity can detect Hg^{2+} ions in water *via* the molecular aggregation and formation of the TDPP–Hg–TDPP complex (Fig. 16). NDPP **21**, on the other hand, operated more efficiently on account of the development of surfactant-free micelle-type ONPs in H_2O. NDPP nanosensors are simple to prepare as compared to other micelle-mediated ONPs. Further, two organic DPP-mediated sensors exhibited excellent selectivity toward Hg^{2+} ions relative to other ions and appropriate solubility in H_2O. In addition, the two sensors exhibited LOD of around 11 nM.

Liu *et al.* recently described ONP mediated on **22** for the fluorescent recognition of Hg^{2+} ions in H_2O.[78] Upon the addition of Hg^{2+}, the nanoparticles of **22** exhibited fluorescence quenching without interference from other metal cations in H_2O (Fig. 16). The LOD was observed to be 4.42 nM for Hg^{2+}. Very recently, pyrazole-based silica-coated magnetite fluorescent nanoprobe **23** was fabricated and investigated for ion detection by Noshin Mir and co-workers (Fig. 16).[79] The investigation of ion detection by synthesized nanoprobe **23** revealed that Hg^{2+} ions in H_2O exhibited one of the highest capacity for fluorescence quenching. Nanoprobe **23** could sense Hg^{2+} with LOD of 7.5 nM and it could be simply isolated from H_2O by means of a bar magnet.

3.6 FON-based chemosensors for iron ions

Iron is the most vital metal ion in the biological system and it plays a crucial role in a variety of chemical processes, *i.e.*, cofactor in enzymatic reactions, cellular metabolism, and transport of oxygen through haem. Its deficiency and excess cause serious disorders in living systems, such as damage to vital organs, anemia, heart failure, and diabetes.[80] Its detection by using the fluorescence technique mainly involves the quenching of emission intensity of the sensor *via* the electron transfer mechanism. However, in some reported cases, fluorescence enhancement is also observed in the fluorophore, which may be caused by the chelation of Fe^{3+}/Fe^{2+} with the fluorophore sensor.[81,82] For the selective sensing of Fe^{3+} in an aqueous medium, a branched nanoreceptor with a triazole as a core and benzothiadiazide derivative as branches (**24**) was fabricated by Wang and co-workers (Fig. 19).[83] The proposed nanosensor exhibited high selectivity and sensitivity toward the targeted ions *via* transformation in the emission profile. The emission of the nanoreceptor quenched by the addition of Fe^{3+} ions was unaffected by the other metal ions. The Fe–organic complex is responsible for such sensing behavior. These selective and promising properties of the nanoreceptor are the key reasons for its application as Fe^{3+} impurity detector in a promising cathode material ($LiFePO_4$) in lithium-ion batteries. The fluorescence intensity of **24** NPs does not show quenching in pure $LiFePO_4$ dissolved in an acid solution, but it gets dramatically quenched when Fe^{3+} impurity is present. The nanosensor can detect Fe^{3+} ions up to 1×10^{-7} M concentration. Similarly, for the detection of Fe^{3+}, naphthalimide FON **25** with aggregation-induced emission enhancement properties were designed and synthesized by Cuiping Han *et al.* (Fig. 19).[84] When excited at 513 nm in a semi-aqueous medium (H_2O: 70%; CH_3CN: 30%), the receptor displayed an emission peak at 523 nm. Fe^{3+} caused an increase in the intensity along with an 8 nm blue-shift in the emission maxima of the nanoreceptor (Fig. 17). The enhancement in the fluorescent intensity along with this blue-shift could be attributed to the inhibition of the PET effect. In the absence of Fe^{3+}, PET takes place from an electron-rich diethylenetriamine unit to an electron-deficient naphthalimide group of receptors; the binding of Fe^{3+} with the lone pair of N from the diethylenetriamine portion resulted in the inhibition of PET and increase in fluorescence. The nanoreceptor exhibited a linear response toward Fe^{3+} ions over a wide concentration range (1 nM to 100 μM) with LOD of 0.35 nM.

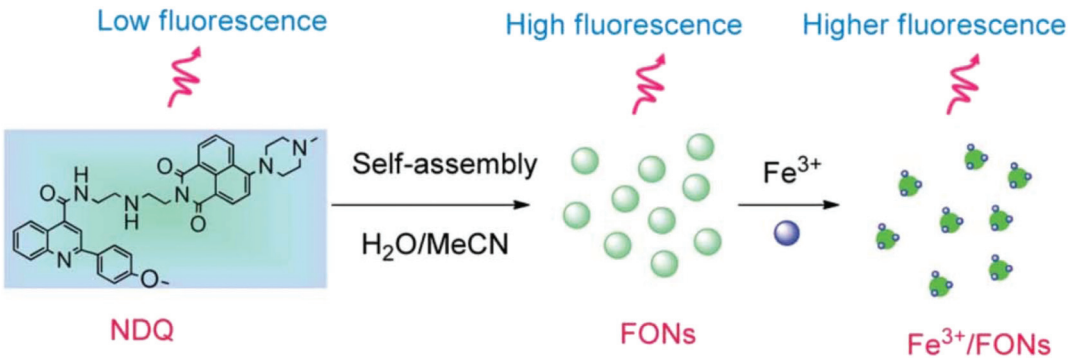

Fig. 17 Schematic illustration of the synthesis of **25** and strategy for Fe^{3+} detection. Adapted with permission from ref. 84. Copyright 2014 the Royal Society of Chemistry.

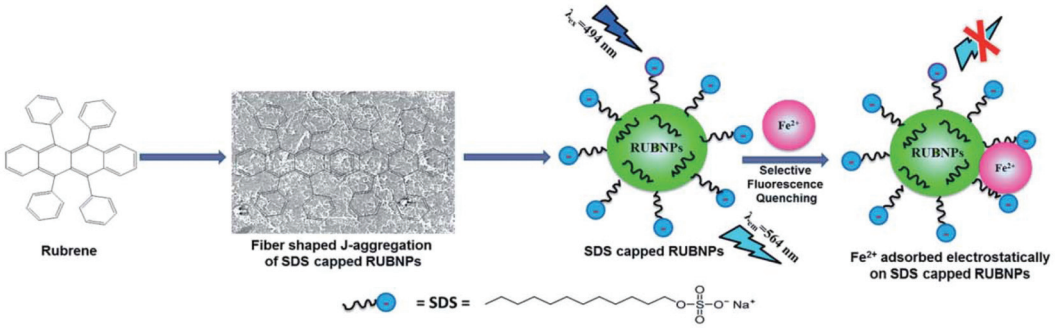

Fig. 18 Plausible fluorescence quenching mechanism based on Fe^{2+} ion adsorption on the surface of SDS-capped RUBNPs. Adapted with permission from ref. 86. Copyright 2015 the Royal Society of Chemistry.

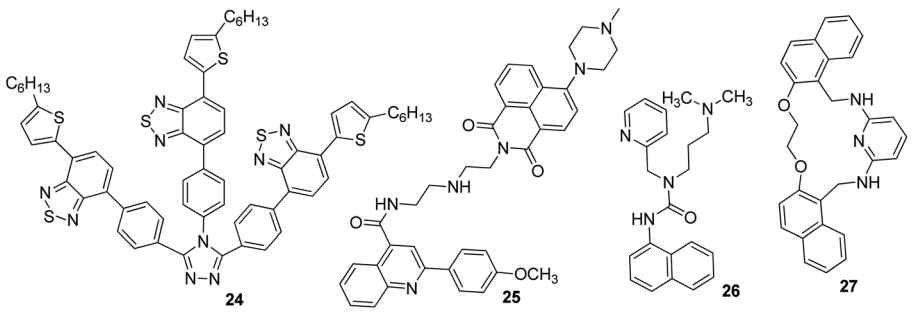

Fig. 19 Structures of FON-based chemosensors for the detection of iron ions.

Tripodal receptor **26** based on organic fluorescent nanoparticles was synthesized by Shweta Chopra *et al.* (Fig. 19).[85] They reported that the fabricated nanoparticles could be used as a Fe^{3+}-selective sensor in aqueous media. Selective fluorescence quenching was observed upon the addition of Fe^{3+} ions with no interference from other metal ions. The lowest detectable concentration of the receptor for Fe^{3+} ions was found to be 1.66 μM. The selective quenching of fluorescence was a result of the inhibition of PET *via* 1 : 1 **26**-Fe^{3+} complex formation. Further, it was observed that spermidine (a biologically active amine) could selectively replace Fe^{3+} ions from **26**-Fe^{3+} and ultimately cause an increase in the fluorescence intensity. On the basis of these observations, a selective detection of spermidine was carried out with LOD of 3.68 μM.

A fluoroionophore sensor based on the sodium dodecyl sulphate (SDS)-capped rubrene nanoparticles (RUBNPs) was reported as a Fe^{2+}-selective chemosensor by Mahajan and coworkers (Fig. 18).[86] The presence of Fe^{2+} in an aqueous suspension of RUBNPs induced fluorescence quenching at 564 nm, and the quenching results fit into a conventional Stern–Volmer relation in the concentration range of 0–80 μg mL^{-1}. The sensor exhibited a good linear relationship toward Fe^{2+} with LOD of 0.015 μg mL^{-1}. Further, the utility of the projected nanosensor was verified through the Fe^{2+} content in a pharmaceutical tablet.

Very recently, Azadbakht and co-workers described a highly stable fluorescent organic sensor mediated on nanoparticles of **27**.[87] This **27**-based chemosensor with a particle size of around 35 nm possesses high selectivity and sensitivity toward Fe^{3+} cations in aqueous buffer solutions as compared to other metal cations such as Ag^{+}, Hg^{2+}, Cd^{2+}, Zn^{2+}, Cu^{2+}, Ni^{2+}, Co^{2+}, Fe^{2+}, Mn^{2+}, Pb^{2+}, Al^{3+}, Ba^{2+}, Ca^{2+}, Mg^{2+}, Cs^{+}, K^{+}, and Na^{+} by fluorescence emission quenching at a wavelength of 358 nm. The LOD of this **27**-based sensor was found to be 5.57 nM for Fe^{3+}.

3.7 FON-based chemosensors for zinc ions

Zinc plays an essential role in pathophysiological processes because of the advantages offered by its structural properties, such as gene expression, cell apoptosis, enzymatic adjustment, and neurotransmission. Some neurological problems like Alzheimer's disease and Parkinson's disease and the pathology of intellectual development is caused by the break-up of zinc homeostasis.[88–90] For the selective detection of zinc ions in an aqueous medium, ONPs with ligand *N*,*N*′-bis(pyridyl-2yl-methyl)ethylenediamine **28** were fabricated by Huerta-Aguilar *et al.* (Fig. 20).[91,92] The fluorescence intensity of the nanorecep-

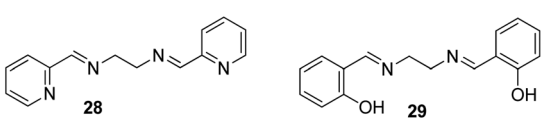

Fig. 20 Structures of FON-based chemosensors for detection of zinc ions.

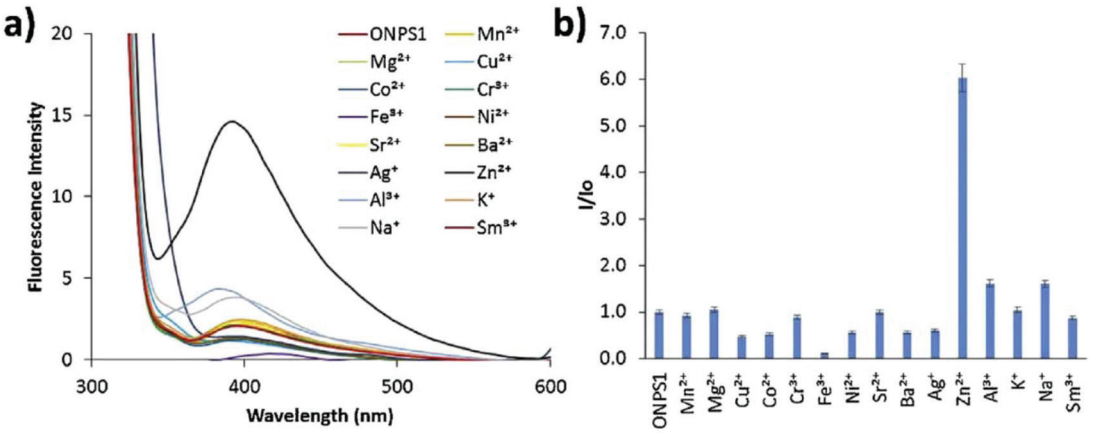

Fig. 21 Fluorescence studies: metal ion binding test for nanoprobe **28** (0.1 mM) in an aqueous medium for the recognition of metal ions; (a) change in fluorescence spectra with respect to different metal ion additions; (b) relative fluorescence intensity at 410 nm against different metal ions. Adapted with permission from ref. 92. Copyright 2016 Elsevier Ltd.

tor increases with the subsequent addition of Zn ions, whereas no enhancement was observed with other common interfering metal ions. The selective response of Zn ions toward nanoprobe **28** was attributed to the inhibition of PET, which was the result Zn-**28** complex formation. The sensor displayed a linear response toward Zn^{2+} (0.0–0.1 mM) with LOD of 470.6 ppb. Further, the scope of the nanosensor was utilized in the determination of Zn^{2+} ions in commercially available multivitamin tablets (Fig. 21). Based on a similar approach, the same group designed the synthesis and fabrication of nanoreceptor **29** for the recognition of Zn^{2+} and Al^{3+} ions in an aqueous medium (Fig. 20). The fluorescence intensity of **29** rose with an increase in the concentration of Zn^{2+}. Interestingly, when Al^{3+} ions were added to **29**-ONPs/Zn^{2+} in a sequential order (addition of Zn^{2+} to **29**-ONPs, followed by Al^{3+}), a further enhancement in the fluorescence with a 50 nm red-shift was observed. The addition of Al^{3+} further activated Zn^{2+}/**29**-ONPs system and induced an increase in fluorescence. The HOMO energy of **29**-Zn^{2+} system is lowered as compared to that of nanoreceptor **29**, which results in the inhibition of PET from the HOMO (donor) to the fluorophore, resulting in an increase in fluorescence. When Al^{3+} is added to the **29**-Zn^{2+} system, the HOMO energy of the receptor gets further stabilized; further, the addition of Al^{3+} causes an increase in the planarity of the complex, leading to strong PET from the receptor, resulting in a further increase in fluorescence.[91,92]

4. FON-based chemosensors for the main group metal ions

4.1 FON-based chemosensors for cesium ions

In a struggle for the development of a Cs^{+} determination technique, **30** was synthesized by Chopra *et al.* by the simple condensation of dipicolinic acid hydrazide with catechol carbaldehyde. In addition, the receptor was fabricated into its nanoparticles to study the ability toward the recognition of Cs^{+} in aqueous media (Fig. 23).[93] Once excited at 309 nm, it showed an emission peak at 412 nm. The emission spectra of the nanoreceptors remained unaffected with most of the other metal ions, *i.e.*, Hg^{2+}, Fe^{3+}, Pb^{2+}, Cd^{2+}, Al^{3+}, Co^{3+}, Zn^{2+}, Ag^{+}, Li^{+}, Sr^{2+}, Ni^{2+}, Cu^{2+}, Mg^{2+}, Ba^{2+}, Mn^{2+}, Na^{+}, K^{+}, Al^{3+}, and Cr^{3+}; however, the addition of Cs^{+} ions caused enhanced emission in the solution with receptor **30** (Fig. 22). This enhancement is expected because of the formation of **1**-Cs^{+} complex, which inhibits the PET effect. The sensitivity experiment showed that the proposed nanosensors could detect Cs^{+} concentrations of up to 70 nm.

4.2 FON-based chemosensors for lithium ions

Due to its smaller size, lithium exhibits high heat of hydration and poor coordination capability; these properties complicate the process of developing selective fluorescent probes for detection.[94,95] However, it possesses high charge density (hard acid), and it can bind with hard donor atoms (oxygen and nitrogen) of the receptor, which may induce changes in the photophysiological properties of the receptor. Therefore, the production of an optical sensor grounded on Biginelli compound **31** fabricated into ONPs *via* the bottom-up technique was formulated by Kaur and co-workers (Fig. 23).[96] There was not a single sort of intrusion from any of the conceivable interfering cations to the proposed nanosensor; however, a stable, rapid, and selective response was exhibited by the nanosensor toward lithium ions. When excited at 300 nm, the nanoreceptor exhibited an emission peak at 353 nm. The emission peak remained unchanged with most of the other metal ions such as Al^{3+}, Na^{+}, Ag^{+}, K^{+}, Cd^{2+}, Cs^{2+}, Pb^{2+}, Mg^{2+}, Hg^{2+}, Ca^{2+}, Zn^{2+}, Sr^{2+}, Cu^{2+}, Ba^{2+}, Co^{2+}, Cr^{2+}, Fe^{3+}, and Mn^{2+}, but a considerable enhancement in the fluorescence intensity was evident after the addition of Li^{+} ions: the LOD was up to 122 nM. The enhancement in fluorescence of the nanoreceptor could be attributed to the ability of Li^{+} to bind with highly electronegative oxygen and nitrogen atoms of the receptor. Moreover, in the practical samples, the working ability of the sensor was

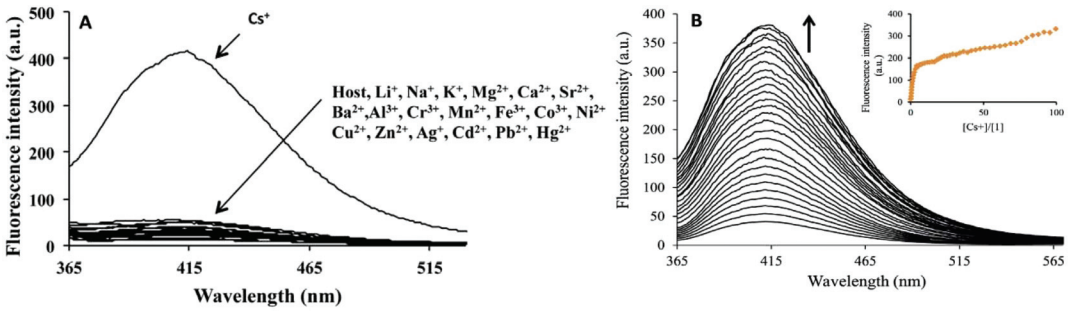

Fig. 22 (A) Changes in fluorescence spectrum of FONs of **30** (1.5 mM) in aqueous media upon the addition of 100 mM of a particular metal nitrate salt in the aqueous medium. (B) Changes in the fluorescence spectrum of FONs of **30** upon the successive addition of Cs^+; inset shows the fluorescence intensity as a function of Cs^+. Adapted with permission from ref. 93. Copyright 2014 Elsevier Ltd.

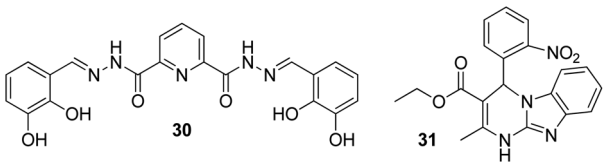

Fig. 23 Structures of FON-based chemosensors for the detection of cesium and lithium ions.

also analyzed through lake and tap waters, and it was observed that the sensor could effectively detect Li^+ ions with an average recovery percentage of 96.5%.

4.3 FON-based chemosensors for strontium ions

Besides many beneficial uses of strontium,[97,98] its one isotope, *i.e.*, radioactive strontium-90, is considered to be one of the "most hazardous" when considering radioactive fallout.[99] There are a few reports on fluorescent probes for the selective detection of strontium.[100,101] Kaur *et al.*[102] synthesized a series of three compounds (**32**, **33**, and **34**), and they fabricated them into ONPs for fluorescent receptor development for detecting cations in aqueous media (Fig. 24). When the synthesized compounds were tested for the detection of different metal ions, only probe **34** displayed an increase in emission when Sr^{2+} was added as a suspected cation. Therefore, for the development of a chemosensor, the deciding factor is the position of the substituent in the organic compound. The fluorescence intensity of the nanosensor increases because the guest molecule binds to the oxygen atom of the carbonyl group (C═O) of compound **34**, which leads to the reduction in the PET process, subsequently leading to fluorescence enhancement.

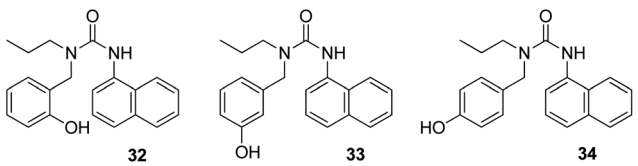

Fig. 24 Structures of FON-based chemosensors for the detection of strontium ions.

The nanosensor proved to be very sensitive toward Sr^{2+}: it could detect Sr^{2+} concentrations as low as 184 μM. Moreover, commercial applications of the sensor were also investigated *via* the determination of Sr^{2+} amount present in toothpastes and oral gels.

4.4 FON-based chemosensors for aluminum ions

Poor coordination ability and lack of spectroscopic characteristics are the two major difficulties in the design of fluorescent probes for the detection of Al^{3+}. The probes that contain strong coordinating groups have been designed for the recognition of Al^{3+}. Based on this, nanoreceptor **36** was synthesized by Saini *et al.*[103] by treating 1,8-naphthalimide with diethylenetriamine (Fig. 25). When excited at 340 nm, the receptor displayed two emission peaks at 340 and 494 nm, respectively. Among the various tested metal ions, Al^{3+} displayed selective enhancement in the emission peak present at 494 nm. The nanosensor exhibited high sensitivity toward Al^{3+} with LOD of 667 nM. Upon the addition of Al^{3+} into a solution containing receptor **36**, Al^{3+} binds with the lone pair of central nitrogen of the diethylenetriamine part of receptor **36** and consumes the excess electron. This results in the reduction of PET and causes an increase in the fluorescence intensity. Based on this same mechanism, Azadbakht and co-workers[104] designed a nanosensor based on macrocycle compound **37**. This nanosensor exhibited an "on–off"-type mode with high selectivity toward Al^{3+} ions (Fig. 25). Upon binding of Al^{3+} with the nanoparticles, a 15-fold fluorescence enhancement at 359 nm was observed. The LOD of **37** for Al^{3+} was as low as 2.8×10^{-7} M. In 2017, Kim and co-workers synthesized water-soluble onion-type ONPs **35** and investigated them for their applicability toward ion detection (Fig. 26).[105] Nanoparticles **35** were in the size range of 4–8 nm and allowed the precise recognition of Al^{3+} ions, even in the presence of higher concentrations of other metal cations: the LOD was 0.76 μM.

4.5 FON-based chemosensors for tin ions

In 2017, Patil and co-workers reported a highly stable fluorescent organic chemosensor based on the nanoparticles of (*E*)-2-((2-phenylhydrazono)methyl)phenol **38** (Fig. 26).[106]

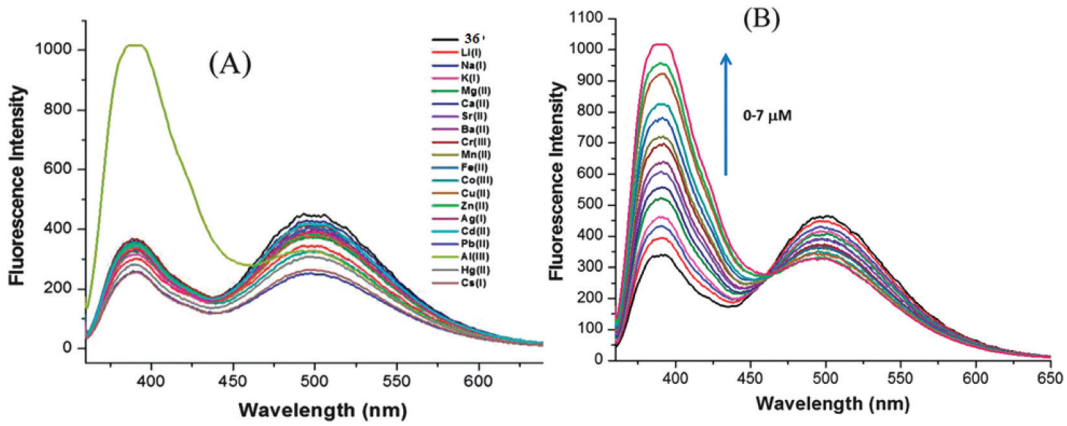

Fig. 25 Changes in the emission profile of nanoaggregates (0.1 mM) in water upon the addition of 20 mM of particular metal nitrate salts. (B) Changes in the emission profile of nanoaggregates (0.1 mM) upon the successive addition of Al^{3+} (0–7 mM). Adapted with permission from ref. 103. Copyright 2014 CNRS and the Royal Society of Chemistry.

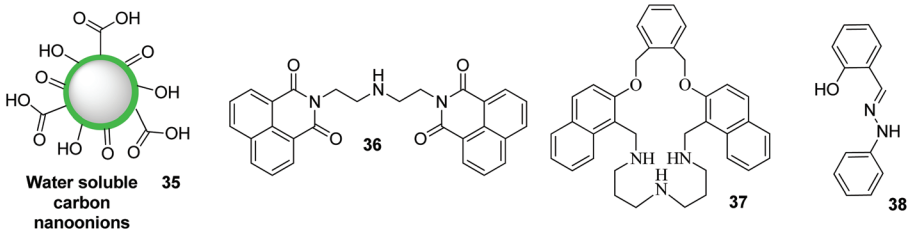

Fig. 26 Structures of FON-based chemosensors for the detection of aluminum and tin ions.

The synthesized PHP-NPs (**38**) were found to have an average size of 93 nm with spherical-shaped morphology. Nanosensors **38** exhibited high selectivity and sensitivity toward the detection of Sn^{2+} cations in H_2O with an increase in fluorescence intensity relative to other cations such as Zn^{2+}, Hg^{2+}, Pb^{2+}, Ca^{2+}, NH^{4+}, Ni^{2+}, Fe^{2+}, Fe^{3+}, and Cu^{2+}, which actually appear to quench the fluorescence of these nanosensors. The LOD was found to be 0.0027 μg mL^{-1}. Further, nanosensors **38** could be utilized to formulate a fluorometric technique for the recognition of Sn^{2+} cations in environmental liquids taken from residential areas. The recognition of Sn^{2+} ions by PHP-NPs yields a purely economical and practical method.

5. Summary of FON properties and comparison with conventional fluorescent chemosensors

The performance summary of FONs is listed in Table 1. Veale and co-workers reviewed conventional fluorescent chemosensors for ions based on organic structures.[107] A comparison between conventional organic chemosensors and nanoparticle-based organic chemosensors revealed that FONs are more valuable and efficient in terms of fluorescence quantum yield, detection limit, decomposition stability, solubility, and thermal stability. From Table 1, it is evident that FONs have lower LOD (0.35 nM), which facilitate high selectivity toward ions even at very low concentrations as compared to other conventional organic chemosensors. The appropriate enhancements in wavelength-shifted fluorescence intensity (238–564 nm) in the case of FONs provided increased amplification of the recognition event. Further, the feature of small-sized nanoparticles (5–222 nm) makes FONs cheaper, noncorrosive, nonflammable, and highly thermally stable as compared to conventional organic chemosensors. Moreover, in comparison with conventional organic chemosensors, FONs have the strongest affinity with the relevant target (binding selectivity); because of this good binding selectivity, the fluorescence signal can avoid environmental interference (signal selectivity), yielding advantages such as sensor ion concentration, photobleaching, environment around the sensor (temperature, polarity, pH, *etc.*), and stability under illumination. In addition, FONs are capable of detecting a large spectrum of ions. On the other hand, traditional chemosensors have a limited range, *i.e.*, there are very rare reports about the use of conventional organic chemosensors in the detection of chromium, strontium, tin, and cesium ions. However, there is still a considerable scope to increase the efficiency and capability of FONs to satisfy various criteria such as fluorescence bioimaging capacity, high biocompatibility, and fast chelation.

Table 1 Summary of sensitivity of various FON-based sensors

Metal ion	Functionalizing agent	Size of nanoparticle (nm)	Detection wavelength (nm)	Mechanism	L.O.D (nM)	Ref.
Ag^{+}	Triazolo-thiadiazole	20	300	PET	258	45
Ag^{+}	1,8-Naphthalimide	25	522 and 627	Formation of excimers	15.5	46
Ag^{+}	Thiourea	100	355	Ag-Nanoparticles on the surface of nanoreceptor	47	48
Ag^{+}	Biginelli	22	350		7.9	51
Cu^{2+}	Pyridinylthiazole	200	525	Adsorption of Cu^{2+} ions to the surface of the nanoparticles	10	53
Cu^{2+}	Cyclen	33–40	540	FRET	340	55
Cu^{2+}	Dihydroxyphenylalanine	160	520	The good selectivity may be due to the binding of Cu^{2+} with N and O atoms on the surface of the PDNPs	100	56
Cr^{6+}	Silole	100	360 and 485	PET	2.187	58
Cr^{6+}	Perylene	34	382	Non-fluorescent micelle complex	8×10^{6}	59
Cr^{6+}	Poly-acrylamide	40	345 and 405	Oxidation of poly-acrylamide	2.0×10^{4}	60
Cr^{3+}	1,8-Naphthalic anhydride	18	500	PET	64	61
Cr^{6+}	1-Pyrenemethylamine	25	238 and 400	PET	2800	62
Cr^{3+}	*N*,*N*′-Bis(5-bromo-2-thiophenylmethyl)ethylenediimine	80	373	PET	7.3×10^{3}	66
Cr^{3+}	Glutathione	69	369 and 400	PET	250	32
Cd^{2+}	Isatin	112	417 and 567	Internal charge transfer (ICT)	1.330×10^{6}	68
Hg^{2+}	Rhodamine	—	530	Spiro lactam ring opening	0.1	69
Hg^{2+}	Thiourea	66	415	PET	2.4	70
Hg^{2+}	Thiourea	200	403	PET	113	71
Hg^{2+}	Biginelli	—	456 and 440	PET	1	73
Hg^{2+}	2-Vinylnaphthalene and acrylic acid	20	365	Complexation reaction	1×10^{4}	74
Hg^{2+}	Hydroxylquinoline	220	400	PET	4.42	78
Hg^{2+}	Pyrazole	10–20	460	PET	7.5	79
Fe^{2+}	Triazole and benzothiadiazide	140	565	Formation of complexes between Fe^{3+} and TAZ-BTTC6	100	82
Fe^{2+}	Naphthalimide	168	513 and 523	PET	0.35	83
Fe^{2+}	Urea	18	370	PET	1660	84
Fe^{2+}	RUBNPs	87.2	564	Formation of a nonfluorescent complex between a fluorophore and Fe^{2+}	1.5×10^{4}	86
Fe^{2+}	2,6-Diaminopyridine Schiff base	35	358	PET	5.57	87
Zn^{2+}	*N*,*N*′-Bis(pyridyl-2yl-methyl)-ethylenediamine	222	365	PET	6.721×10^{4}	91
Cs^{+}		65–90	412	PET	70	92
Li^{+}	Biginneli	25	353	PET	122	95
Sr^{2+}	Urea	5–10	380	PET	184 000	101
Al^{3+}	1,8-Naphthalimide with diethylenetriamine	55	494	PET	667	102
Al^{3+}		50	359	PET	280	104
Sn^{2+}	(*E*)-2-((2-Phenylhydrazono)methyl)-phenol	93	532 and 552	Excited state complexation formation	0.218	106

L.O.D = Limit of detection; nm = nanometer; nM = nanomolar.

6. Conclusion and outlook

In conclusion, the toxic effects of metal ions in the environment, particularly in water, have urged chemists and biologists to design probes for monitoring these ions. Due to the ease of preparation, high selectivity and sensitivity, ease of operation, and less toxicity, the fabrication of FONs has proven to be an ideal, effective, and straightforward methodology for the detection of metal ions in aqueous media in the recent years. The objective of this review was to summarize the recent developments in the area of FON-based chemosensors to motivate researchers for planning and constructing a new library of such chemosensors having improved selectivity and sensitivity. Following are some of the properties of an ideal FON-based chemosensor: (i) cheap (ease of preparation/fabrication); (ii) long-lasting stability under humidity and atmospheric oxygen;(iii) noncorrosive, nonflammable, and highly thermally stable; (iv) stable toward base and acid hydrolysis actions; (v) excellent solubility in water and other organic solvents; (vi) promising selectivity and sensitivity at lower concentrations; (vii) stable toward oxidative and reductive decompositions; (viii) appropriate detection limit; (ix) appropriate fluorescence quantum yield; (x) ineffective toward impurities in the aqueous media; and (xi) quick response toward ion presence. This area of research has opened up new avenues in the field of nanotechnology/supra-

molecular chemistry and can attract increased attention from chemists and biologists in the future.

Conflicts of interest

There are no conflicts to declare.

References

1 D. T. Quang and J. S. Kim, *Chem. Rev.*, 2010, **110**, 6280–6301.
2 G. P. Rao, C. Lu and F. Su, *Sep. Purif. Technol.*, 2007, **58**, 224–231.
3 F. P. Guengerich, *J. Biol. Chem.*, 2009, **284**, 709.
4 J. J. Lacroix, F. V. Campos, L. Frezza and F. Bezanilla, *Neuron*, 2013, **79**, 651–657.
5 E. Boopathi, J. A. Hypolite, S. A. Zderic, C. M. Gomes, B. Malkowicz, H.-C. Liou, A. J. Wein and S. Chacko, *Mol. Cell. Biol.*, 2013, **33**, 1085–1102.
6 P. C. Tizioto, C. F. Gromboni, A. R. de Araujo Nogueira, M. M. de Souza, M. de Alvarenga Mudadu, P. Tholon, A. do Nascimento Rosa, R. R. Tullio, S. R. Medeiros and R. T. Nassu, *Meat Sci.*, 2014, **96**, 436–440.
7 M. Csuros and C. Csuros, *Environmental sampling and analysis for metals*, CRC Press, 2016.
8 J. A. Lemire, J. J. Harrison and R. J. Turner, *Nat. Rev. Microbiol.*, 2013, **11**, 371.
9 K. P. Carter, A. M. Young and A. E. Palmer, *Chem. Rev.*, 2014, **114**, 4564–4601.
10 M. Bauer and S. Döpfmer, *J. Clin. Psychopharmacol.*, 1999, **19**, 427–434.
11 P. K. Whelton, J. He, J. A. Cutler, F. L. Brancati, L. J. Appel, D. Follmann and M. J. Klag, *J. Am. Med. Assoc.*, 1997, **277**, 1624–1632.
12 S. C. Bondy, *Neurotoxicology*, 2016, **52**, 222–229.
13 N. D. Barnard, A. I. Bush, A. Ceccarelli, J. Cooper, C. A. de Jager, K. I. Erickson, G. Fraser, S. Kesler, S. M. Levin and B. Lucey, *Neurobiol. Aging*, 2014, **35**, S74–S78.
14 K. Hirose, *Anal. Sci.*, 2006, **22**, 1055–1063.
15 F. M. M. Morel and N. M. Price, *Science*, 2003, **300**, 944–947.
16 F. Fu and Q. Wang, *J. Environ. Manage.*, 2011, **92**, 407–418.
17 F. Ge, M.-M. Li, H. Ye and B.-X. Zhao, *J. Hazard. Mater.*, 2012, **211**, 366–372.
18 M. Al-Shannag, Z. Al-Qodah, K. Bani-Melhem, M. R. Qtaishat and M. Alkasrawi, *Chem. Eng. J.*, 2015, **260**, 749–756.
19 M. Ghaedi, F. Ahmadi and A. Shokrollahi, *J. Hazard. Mater.*, 2007, **142**, 272–278.
20 M. Arienzo and R. Capasso, *J. Agric. Food Chem.*, 2000, **48**, 1405–1410.
21 J. Wu, J. Yu, J. Li, J. Wang and Y. Ying, *Spectrochim. Acta, Part B*, 2007, **62**, 1269–1272.
22 R. S. Houk, V. A. Fassel, G. D. Flesch, H. J. Svec, A. L. Gray and C. E. Taylor, *Anal. Chem.*, 1980, **52**, 2283–2289.
23 A. Montaser, *Inductively coupled plasma mass spectrometry*, John Wiley & Sons, 1998.
24 S. Hirata, Y. Umezaki and M. Ikeda, *Anal. Chem.*, 1986, **58**, 2602–2606.
25 F. J. Hayes, H. B. Halsall and W. R. Heineman, *Anal. Chem.*, 1994, **66**, 1860–1865.
26 C. C. Chang, *Surf. Sci.*, 1971, **25**, 53–79.
27 T. M. Florence, *Analyst*, 1986, **111**, 489–505.
28 J. F. Zhang, Y. Zhou, J. Yoon and J. S. Kim, *Chem. Soc. Rev.*, 2011, **40**, 3416–3429.
29 Y.-L. Hung, T.-M. Hsiung, Y.-Y. Chen, Y.-F. Huang and C.-C. Huang, *J. Phys. Chem. C*, 2010, **114**, 16329–16334.
30 H. N. Kim, W. X. Ren, J. S. Kim and J. Yoon, *Chem. Soc. Rev.*, 2012, **41**, 3210–3244.
31 J. S. Kim and D. T. Quang, *Chem. Rev.*, 2007, **107**, 3780–3799.
32 N. Kaur, S. Kaur, R. Mehan, C. A. H. Aguilar, P. Thangarasu and N. Singh, *Sens. Actuators, B*, 2015, **206**, 90–97.
33 A. N. Uglov, A. Bessmertnykh-Lemeune, R. Guilard, A. D. Averin and I. P. Beletskaya, *Russ. Chem. Rev.*, 2014, **83**, 196.
34 B.-K. An, S.-K. Kwon, S.-D. Jung and S. Y. Park, *J. Am. Chem. Soc.*, 2002, **124**, 14410–14415.
35 X. Zhang, S. Wang, L. Xu, L. Feng, Y. Ji, L. Tao, S. Li and Y. Wei, *Nanoscale*, 2012, **4**, 5581–5584.
36 Y.-Y. Sun, J.-H. Liao, J.-M. Fang, P.-T. Chou, C.-H. Shen, C.-W. Hsu and L.-C. Chen, *Org. Lett.*, 2006, **8**, 3713–3716.
37 A. Patra, C. G. Chandaluri and T. P. Radhakrishnan, *Nanoscale*, 2012, **4**, 343–359.
38 H. Kasai, H. S. Nalwa, H. Oikawa, S. Okada, H. Matsuda, N. Minami, A. Kakuta, K. Ono, A. Mukoh and H. Nakanishi, *Jpn. J. Appl. Phys.*, 1992, **31**, L1132.
39 Y. Bai, H. Xing, G. A. Vincil, J. Lee, E. J. Henderson, Y. Lu, N. G. Lemcoff and S. C. Zimmerman, *Chem. Sci.*, 2014, **5**, 2862–2868.
40 W. Cheng, L. Capretto, M. Hill and X. Zhang, *Nanotechnol. Life Sci.*, 2015, **104**, 221–257.
41 T. Asahi, T. Sugiyama and H. Masuhara, *Acc. Chem. Res.*, 2008, **41**, 1790–1798.
42 Y. Zhou, C.-Y. Zhu, X.-S. Gao, X.-Y. You and C. Yao, *Org. Lett.*, 2010, **12**, 2566–2569.
43 L. He, B. Dong, Y. Liu and W. Lin, *Chem. Soc. Rev.*, 2016, **45**, 6449–6461.
44 S. Martin and W. Griswold, *Environ. Sci. Technol. Briefs Citizens*, 2009, **15**, 1–6.
45 A. Chatterjee, M. Santra, N. Won, S. Kim, J. K. Kim, S. Bin Kim and K. H. Ahn, *J. Am. Chem. Soc.*, 2009, **131**, 2040–2041.
46 H. Yan, H. Su, D. Tian, F. Miao and H. Li, *Sens. Actuators, B*, 2011, **160**, 656–661.
47 H. Sharma, V. K. Bhardwaj and N. Singh, *Eur. J. Inorg. Chem.*, 2014, **2014**, 5424–5431.
48 R. G. Pearson, *J. Am. Chem. Soc.*, 1963, **85**, 3533–3539.

49 R. G. Pearson and J. Songstad, *J. Am. Chem. Soc.*, 1967, **89**, 1827–1836.
50 F. Qu, J. Liu, H. Yan, L. Peng and H. Li, *Tetrahedron Lett.*, 2008, **49**, 7438–7441.
51 G. Kaur, T. Raj, S. Singhal and N. Kaur, *Sens. Actuators, B*, 2018, **255**, 424–432.
52 M. B. Gumpu, S. Sethuraman, U. M. Krishnan and J. B. B. Rayappan, *Sens. Actuators, B*, 2015, **213**, 515–533.
53 H. Qin, J. Ren, J. Wang and E. Wang, *Chem. Commun.*, 2010, **46**, 7385–7387.
54 J. Hou, L.-Y. Wang, D.-H. Li and X. Wu, *Tetrahedron Lett.*, 2011, **52**, 2710–2714.
55 R. M. Duke, E. B. Veale, F. M. Pfeffer, P. E. Kruger and T. Gunnlaugsson, *Chem. Soc. Rev.*, 2010, **39**, 3936–3953.
56 J. Chen, Y. Li, W. Zhong, Q. Hou, H. Wang, X. Sun and P. Yi, *Sens. Actuators, B*, 2015, **206**, 230–238.
57 Y. Su, B. Shi, S. Liao, Y. Qin, L. Zhang, M. Huang and S. Zhao, *Sens. Actuators, B*, 2016, **225**, 334–339.
58 A. Zhitkovich, *Chem. Res. Toxicol.*, 2011, **24**, 1617–1629.
59 S. J. Toal, K. A. Jones, D. Magde and W. C. Trogler, *J. Am. Chem. Soc.*, 2005, **127**, 11661–11665.
60 D. K. Dalavi, D. P. Bhopate, A. S. Bagawan, A. H. Gore, N. K. Desai, A. A. Kamble, P. G. Mahajan, G. B. Kolekar and S. R. Patil, *Anal. Methods*, 2014, **6**, 6948–6955.
61 L. Wang, T. Xia, J. Liu, L. Wang, H. Chen, L. Dong and G. Bian, *Spectrochim. Acta, Part A*, 2005, **62**, 565–569.
62 A. Saini, A. K. K. Bhasin, N. Singh and N. Kaur, *New J. Chem.*, 2016, **40**, 278–284.
63 X. Zhang, X. Zhang, W. Shi, X. Meng, C. Lee and S. Lee, *J. Phys. Chem. B*, 2005, **109**, 18777–18780.
64 Y. Zhou, F. Wang, Y. Kim, S.-J. Kim and J. Yoon, *Org. Lett.*, 2009, **11**, 4442–4445.
65 L. Wang, L. Wang, T. Xia, L. DONG, G. BIAN and H. CHEN, *Anal. Sci.*, 2004, **20**, 1013–1017.
66 P. B. Viviana, C. A. Huerta-Aguilar, N. Singh and T. Pandiyan, *Res. Chem. Intermed.*, 2018, **44**, 3179–3197.
67 H. J. Jung, N. Singh and D. O. Jang, *Tetrahedron Lett.*, 2008, **49**, 2960–2964.
68 P. Saluja, V. K. Bhardwaj, T. Pandiyan, S. Kaur, N. Kaur and N. Singh, *RSC Adv.*, 2014, **4**, 9784–9790.
69 P. G. Mahajan, D. P. Bhopate, G. B. Kolekar and S. R. Patil, *Sens. Actuators, B*, 2015, **220**, 864–872.
70 V. K. Bhardwaj, H. Sharma, N. Kaur and N. Singh, *New J. Chem.*, 2013, **37**, 4192–4198.
71 A. Singh, S. Kaur, N. Singh and N. Kaur, *Org. Biomol. Chem.*, 2014, **12**, 2302–2309.
72 H. Li and H. Yan, *J. Phys. Chem. C*, 2009, **113**, 7526–7530.
73 A. Corsaro and V. Pistara, *Tetrahedron*, 1998, **54**, 15027–15062.
74 A. Singh, T. Raj, T. Aree and N. Singh, *Inorg. Chem.*, 2013, **52**, 13830–13832.
75 L. Wang, L. Dong, G.-R. Bian and T.-T. Xia, *Spectrochim. Acta, Part A*, 2005, **62**, 313–316.
76 H. Wang, P. Zhang, J. Chen, Y. Li, M. Yu, Y. Long and P. Yi, *Sens. Actuators, B*, 2017, **242**, 818–824.
77 K. Nie, B. Dong, H. Shi, Z. Liu and B. Liang, *Anal. Chem.*, 2017, **89**, 2928–2936.
78 L.-N. Liu, L. He, Y. Qu, N. Lu, Q.-Y. Cao and Z. Yan, *Inorg. Chim. Acta*, 2018, **474**, 128–133.
79 N. Mir, A. Heidari, H. Beyzaei, S. Mirkazehi-Rigi and P. Karimi, *Chem. Eng. J.*, 2017, **327**, 648–655.
80 P. Ponikowski, D. J. Van Veldhuisen, J. Comin-Colet, G. Ertl, M. Komajda, V. Mareev, T. McDonagh, A. Parkhomenko, L. Tavazzi and V. Levesque, *Eur. Heart J.*, 2014, **36**, 657–668.
81 B. P. Espósito, S. Epsztejn, W. Breuer and Z. I. Cabantchik, *Anal. Biochem.*, 2002, **304**, 1–18.
82 S. K. Sahoo, D. Sharma, R. K. Bera, G. Crisponi and J. F. Callan, *Chem. Soc. Rev.*, 2012, **41**, 7195–7227.
83 J. Wang, X. Xu, L. Shi and L. Li, *ACS Appl. Mater. Interfaces*, 2013, **5**, 3392–3400.
84 C. Han, T. Huang, Q. Liu, H. Xu, Y. Zhuang, J. Li, J. Hu, A. Wang and K. Xu, *J. Mater. Chem. C*, 2014, **2**, 9077–9082.
85 S. Chopra, J. Singh, H. Kaur, H. Singh, N. Singh and N. Kaur, *New J. Chem.*, 2015, **39**, 3507–3512.
86 P. G. Mahajan, D. P. Bhopate, A. A. Kamble, D. K. Dalavi, G. B. Kolekar and S. R. Patil, *Anal. Methods*, 2015, **7**, 7889–7898.
87 R. Azadbakht, M. Hakimi and J. Khanabadi, *New J. Chem.*, 2018, **42**, 5929–5936.
88 T. Kambe, T. Tsuji, A. Hashimoto and N. Itsumura, *Physiol. Rev.*, 2015, **95**, 749–784.
89 S. M. Y. Kong, B. K. K. Chan, J.-S. Park, K. J. Hill, J. B. Aitken, L. Cottle, H. Farghaian, A. R. Cole, P. A. Lay and C. M. Sue, *Hum. Mol. Genet.*, 2014, **23**, 2816–2833.
90 P. Jiang and Z. Guo, *Coord. Chem. Rev.*, 2004, **248**, 205–229.
91 C. A. Huerta-Aguilar, T. Pandiyan, P. Raj, N. Singh and R. Zanella, *Sens. Actuators, B*, 2016, **223**, 59–67.
92 C. A. Huerta-Aguilar, T. Pandiyan, N. Singh and N. Jayanthi, *Spectrochim. Acta, Part A*, 2015, **146**, 142–150.
93 S. Chopra, N. Singh, P. Thangarasu, V. K. Bhardwaj and N. Kaur, *Dyes Pigm.*, 2014, **106**, 45–50.
94 S. Rochat, Z. Grote and K. Severin, *Org. Biomol. Chem.*, 2009, **7**, 1147–1153.
95 J. Gao, S. Rochat, X. Qian and K. Severin, *Chem. – Eur. J.*, 2010, **16**, 5013–5017.
96 G. Kaur, A. Singh, P. Venugopalan, N. Kaur and N. Singh, *RSC Adv.*, 2016, **6**, 1792–1799.
97 W. E. Cabrera, I. Schrooten, M. E. De Broe and P. C. d'Haese, *J. Bone Miner. Res.*, 1999, **14**, 661–668.
98 R. H. Wasserman, *Clin. Chem.*, 1998, **44**, 437–439.
99 T. Fukuda, F. Arai and M. Nakajima, *Micro-nanorobotic manipulation systems and their applications*, Springer Science & Business Media, 2013.
100 H.-F. Ji, Y. Yang, X. Xu and G. Brown, *Org. Biomol. Chem.*, 2006, **4**, 770–772.
101 A. Kaur, G. Kaur, A. Singh, N. Singh and N. Kaur, *ACS Sustainable Chem. Eng.*, 2015, **4**, 94–101.

102 S. Kaur, A. Kaur, N. Kaur and N. Singh, *Org. Biomol. Chem.*, 2014, **12**, 8230–8238.
103 A. Saini, J. Singh, R. Kaur, N. Singh and N. Kaur, *New J. Chem.*, 2014, **38**, 4580–4586.
104 R. Azadbakht, M. Talebi, J. Karimi and R. Golbedaghi, *Inorg. Chim. Acta*, 2016, **453**, 728–734.
105 K. M. Tripathi, T. S. Tran, Y. J. Kim and T. Kim, *ACS Sustainable Chem. Eng.*, 2017, **5**, 3982–3992.
106 K. S. Patil, P. G. Mahajan and S. R. Patil, *Spectrochim. Acta, Part A*, 2017, **170**, 131–137.
107 E. B. Veale and T. Gunnlaugsson, *Annu. Rep. Prog. Chem., Sect. B: Org. Chem.*, 2010, **106**, 376–406.